

Basic design limitations for urban electric VTOL aircraft

Olivier Cornes

Conceptual aircraft designer
Aurora Swiss Aerospace
6004 Luzern, Switzerland

PLEASE NOTE: DO NOT INCLUDE EMAIL ON 1ST PAGE

ABSTRACT

Urban air mobility has the potential to change the face of aeronautics and transportation, which has created a lot of speculation on what the new technology is capable of. The uncertainty is increased by the fact that urban air mobility is an unchartered field of aeronautics and the proposed designs vary significantly, especially because of new technologies such as distributed electric propulsion which give extreme design freedom. However, there exist a short series of simple physical rules that set limits on what can be done in order to meet stringent constraints of urban eVTOLs, such as noise, range, and payload requirements. This work aims at showing these limits, especially with regards to aircraft footprint and noise, and what technological and physical parameters drive these limits. The method employed uses an original but simple mathematical model to size eVTOLs for a variety of missions based on extensive quantities only, such as power required for flight, battery capacity and empty weight fraction. The assembly of these comparatively simple equations reduces down to solving a quartic equation for sizing an aircraft, which is done rapidly and robustly with a current desktop computer, and thus allows for extensive design space exploration. Using this tools, this work investigates the effects of increasing range, payload, and footprint of eVTOL aircraft for urban transportation needs. It is found that the rotor area to footprint ratio should be greater than 0.2 to avoid large mass penalties due to excessive power requirements. Also, smaller footprint vehicle require relatively larger rotors to be feasible. Main drivers for the take-off noise is found to be footprint, whereas improved battery technology has negligible effect on noise.

*

Nomenclature

A_i	A-weighting for harmonic i [-]	m_{bat}	mass of battery [kg]
B	number of rotor blades [-]	m_{empty}	dry mass of vehicle (no payload, fuel or battery) [kg]
b	fixed wing span [m]	m_i	harmonic i [-]
$C_{d,0}$	parasitic drag coefficient [-]	$m_{payload}$	mass of payload [kg]
D	drag [N]	M_t	tip mach number [-]
d_{cruise}	cruise distance [m]	P_v	hover power [W]
e	span efficiency [-]	P_h	power absorbed by rotor [hp]
$eVTOL$	electric vertical take-off and landing	P_{ref}	sound reference pressure [Pa]
E_{climb}	energy required for climb [J]	$p_{m,i}$	sound pressure level of i th harmonic [-]
E_{cruise}	energy required for cruise [J]	q	dynamic pressure [Pa]
E_{tot}	total energy [J]	Re	reynolds number [-]
FOM	Figure of merit [-]	R	rotor diameter [ft]
g	Gravity acceleration [m/s]	r	distance to observer [ft]
$GTOW$	Gross take off weight [kg]	S_d	vertical propulsion disc area [m^2]
h_c	height of climb segment (cruise regime) [m]	S_{ref}	fixed wing area [m^2]
h_v	height in vertical flight regime [m]	t_v	time in vertical flight regime [s]
$J_{m_iB}(x)$	Bessel function of order m_iB at distance x [-]	T	thrust [N]
k_{empty}	vehicle empty mass fraction [-]	UAV	Unmanned Aerial Vehicle
m_{tot}	mass of complete vehicle [kg]	v_{cruise}	cruise velocity [m/s]
$MTOW$	Maximum take off weight [kg]	$VTOL$	vertical take-off and landing
		η_s	structural mass fraction [-]
		η_p	forward propulsion efficiency [-]
		η_e	electric power train efficiency [-]
		μ	air dynamic viscosity [$kg/m/s$]
		ρ	air density [kg/m^3]
		θ	angle between observer and propeller axis [degrees]

Presented at the Vertical Flight Society 75th Annual Forum & Technology Display, Philadelphia, Pennsylvania, May 13–16, 2019.
Copyright © 2019 by AHS - The Vertical Flight Society. All rights reserved.

INTRODUCTION

Urban air mobility has been a genuine engineering pursuit since the 1960s and 1970s (Ref. 1). In recent years, many companies are investing in serious efforts to make urban air mobility a reality (Refs. 2–4). The unconventional design space afforded by urban air mobility has sprouted a wide variety of new aircraft concepts. The affluence of new aeronautical creations may lead to think that limits on aeronautical sciences are being lifted and that any form of urban air mobility is possible: extreme ranges, small aircraft footprints, and large payloads are often promised. Moreover, aeronautical companies invest large amounts of effort in finding the aircraft configurations that will satisfy all the requirements.

However, even with improving technologies, there are physical limits that can not be exceeded. This study explores some of these limits, to show whether any aircraft configuration has a chance of meeting a particular set of requirements. This work is analogous to an algebraic proof showing the non-existence of a solution.

Although distributed electric propulsion allows for a very broad design space, there are recurring features which are common to all eVTOLs:

- The propulsion system has a dual mode: a hovering or short take-off mode, and a cruising mode. Both modes may be handled by the same propulsion system (such as tilting mechanisms or lift augmentation systems) or separate ("lift and cruise" propulsion).
- All the VTOL aircraft considered have a dual mode lifting system, that is a lifting system for hovering (or short take-off mode), which is analogous to a set of rotors or an augmented wing, and a cruise mode (usually a wing based system, such as a flying wing, a tandem wing, or wing and tail).
- All the VTOL aircraft considered use light-weight technologies (such as composite structures)

By using these assumptions, a basic mathematical model is constructed to describe the design of an eVTOL. It must be simple enough to understand it and explore it fully. Hence the approach is to focus on first-principle equations and cluster all design and implementation aspects into few coefficients and constants. The choice of these constants is based on historical data of existing VTOL aircraft and more generally all aircraft that share the characteristics of interest.

This study is articulated around the following metrics:

Noise Previous experience (Ref. 1) suggests that it is noise that prevented the adoption of urban air commutes in the 1960's and 1970's. Community acceptance is still a significant challenge today for helicopter airlines (Ref. 5). This shows how sensitive the eVTOL market is to the noise the vehicles generate.

Footprint The second aspect that is specific to and drives the eVTOL market is the vehicle footprint: a large vehicle,

even if it has VTOL capability, has more limited landing opportunities than a small one. As can be seen in most eVTOL projects, the vehicle footprint is small in comparison to traditional air vehicles.

A small footprint is critical for projects that aim at producing personal aerial vehicles which the customer would have to store on his/her property (Ref. 6).

Maximum take-off weight The last key metric considered in this study is the maximum take-off gross weight, which is often a surrogate for vehicle cost. This is a key parameter for mass adoption, which the eVTOL paradigm relies upon.

The paper is constructed as follows: first, a description of the mathematical model is given. The model consists of two parts, the vehicle model and the mission model.

The second part presents the results of running this model: first, it is used to verify some assumptions that were made in building it, and then the results from which the conclusions are drawn.

The third part interprets the results and opens on a series of questions and suggestions concerning eVTOL design for a profitable urban air mobility market.

MATHEMATICAL DESCRIPTION

The aim of this work is to gain insight into the limitations of urban eVTOL design: this is done through the setup of a comparatively simple mathematical model with strong but few assumptions so that causes and observations can be easily traced. The mathematical model is a sizing process: it produces a maximum take-off weight for a vehicle with a specified mission if that vehicle is possible according to the assumptions. The sizing process has mass-build up assumptions, aerodynamic assumptions, and mission assumptions presented in order below:

Mass build-up

$$m_{tot} = m_{bat} + m_{empty} + m_{payload} \quad (1)$$

$$m_{tot} = m_{bat} + k_{empty}m_{tot} + m_{payload} \quad (2)$$

Where m_{bat} is given depending on the energy spent for the mission, the empty mass is a function of the total aircraft mass based on historical mass build-ups as described in the following section, and the payload mass $m_{payload}$ is whatever is left to close the equation.

The key parameter in this model is the empty mass fraction k_{empty} . As it turns out, this fraction is in a relatively narrow range for a wide range of different aircraft, as shown in Figure .1. The reference value for the mass fraction chosen for this work is $k_{empty} = 0.65$.

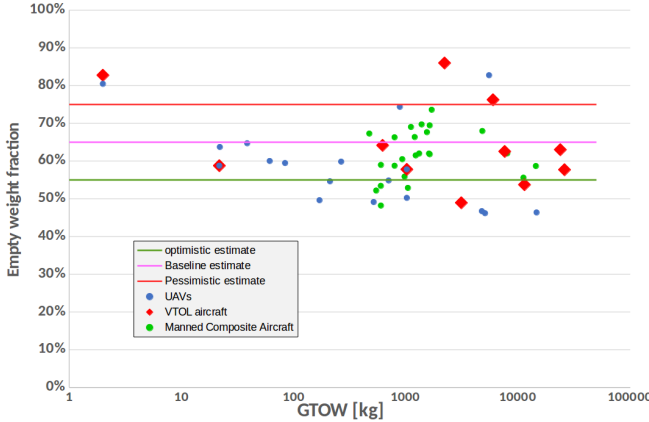


Fig. 1: *Empty mass fraction of a range of different aircraft.* Note that despite radically different purposes (UAVs, general aviation or vertical take-off and landing) the empty mass fraction is for the most part confined in the 0.55 to 0.75 band. The VTOL exceptions to this rule are the Harrier jump jet ($k_{empty} = 54\%$) and the MD900 helicopter ($k_{empty} = 49\%$). Note that the MD900 helicopter only has a single hover and cruise flight system, it rotor. VTOL concepts that have dual propulsion or tilting mechanisms tend are heavier. All aircraft represented here can be found in the table the appendix

Battery model

The battery model linking the energy required to fly the mission to the battery weight is simple:

$$m_{bat} = \frac{E_{tot}}{\rho_{bat}} \quad (3)$$

Note however that there exists a maximum power draw on a given battery. In order to be consistent with industry practice, the power draw is expressed in terms of C-rate:

$$C [1/h] = \frac{\text{Electrical power draw [kW]}}{\text{Battery capacity [kWh]}} \quad (4)$$

Maximum C-rate decreases with increasing energy density. Increased power draw also limits battery life. For lithium cells, a typical value for energy density is 140 Wh/kg at battery level. The reference case here assumes improved batteries at 200 Wh/kg. The maximum C-rate assumed here is 10 C. No assumption is made on the battery technology except for the choice of energy density and maximum allowable C-rate.

Aerodynamic performance model for cruise and climb

Assumption here is that the span of the vehicle for wing-born cruise b is given by the diameter of the footprint. The drag is modeled as a parabolic function:

$$D = qS_{ref}C_{D,0} + \frac{0.074}{\left(\frac{\rho_{vcruise}S_{ref}}{\mu b}\right)^{0.2}}S_{ref} + \frac{m_{tot}^2 g^2}{\pi e b^2 q} \quad (5)$$

With the first term being the parasitic drag, the middle term being the viscous drag contribution modeled as the skin friction drag of a turbulent flat plate and the third term being the induced drag.

The parasitic drag is calculated through the wing area, dynamics pressure and the parasitic drag coefficient. The use of the wing area as a surrogate for the entire vehicle area is misleading for small wing areas, since a real vehicle has a fuselage and other bodies whose contribution becomes significant when the wing becomes small. The drag coefficient chosen here as a baseline is $C_{d,0} = 0.03$, which is similar to that of a Cessna 172 Skyhawk ($C_{d,0} = 0.032$, (Ref. 7)). Although it can be argued that the Skyhawk is an old airplane, eVTOLs will have more protuberances due to vertical lift propulsion systems than a clean aircraft despite advanced aerodynamic design. As will be seen at the end of this section, parasitic drag has little effect for the ranges considered for eVTOL.

As can be seen in the mission model, there is a climb segment and a descent segment. Since the climb angle and climb distance are relatively small in comparison to classical aircraft, the energy required for the entire segment is assumed to be that of the level cruise plus the potential energy the aircraft has to acquire to lift itself to the cruise altitude. Although this energy is recovered in part during descent, we will assume in this case that it is not to provide a conservative estimate of the energy required for the entire segment. The level cruise drag and potential energy give us the energy required for the cruise segment:

$$E_{cruise} = \frac{1}{\eta_p} (Dd_{cruise} + m_{tot}g(h_c - h_v)) \quad (6)$$

Aerodynamic performance model for vertical take-off and landing

The energy required for vertical flight is calculated using a hover time t_v and a hover power and height of vertical flight h_v :

$$E_{vertical} = m_{tot}gh_v + t_v P_v \quad (7)$$

This approximation is consistent with eVTOL vehicles, which have relatively little vertical speeds in hover (Ref. 8). The hover power is given by the equation below, which stems from momentum theory (Ref. 8):

$$P_v = \frac{(m_{tot}g)^{3/2}}{\sqrt{2\rho S_d FOM}} \quad (8)$$

Mission model

An urban transportation application will have the following characteristics:

Short or vertical take-off and landing For a generic urban mission such as the ones considered by (Refs. 2–4, 6, 9) on eVTOLs, there is a necessity to land and take off in enclosed spaces. These might afford enough space for short take-off and landings, but not the space of an airport, requiring the aircraft to land substantially outside of the urban areas, which defeats the mission purpose.

Small climb and descent segments Unlike classical airplanes, eVTOLs will have short climb and descent segments. This statement is based on the two following assumptions: first, eVTOLs by definition will not use jet engines, making climbing to high altitudes useless for propulsion reasons. Second, unlike general aviation aircraft, eVTOLs will require sophisticated navigation and collision avoidance systems to navigate the urban environment. Thus flying relatively low will not pose an issue for collision or navigation purposes.

Contain transitions Since the vehicle will be transitioning from a vertical or near vertical flight to a horizontal flight, the mission will contain a transition segment of one type or another.

A typical eVTOL mission is depicted on Figure 2. According to (Refs. 2–4,9), typical eVTOL missions will have ranges between 50 and 150 km, and cruise heights around 500 m AGL. The height of the take-off segment has to be high enough to clear urban obstacles. The reference value is fixed to 100 m. The influence of this parameter is discussed at the end of this section. The payload is variable, depending on the number of passengers. For this study, we will consider a lower bound of 1 passengers (100 kg) and an upper bound of 4 passengers (400 kg). According to (Ref. 2), the cruise speed of the vehicle should be situated between 150 and 200 mph (240 and 320 km/h). These velocities are unpractical for current and near-future technologies, as will be shown subsequently. Although the upper bound is left as is, the lower bound is brought down to 200 km/h. The reference speed is chosen to be 250 km/h. The typical mission profile is shown below in terms of power profile: it consists of a take-off phase (in which transition is included), a cruise segment and a landing segment. Some simplifying assumptions are made here:

- The outbound and the inbound transition is smooth enough that it does not require more than the take-off power to do so. It is also assumed that the vehicle is properly designed for transition, i.e. the transition is done with negligible energy for the overall mission and the peak power during the transition is a moderate increase with respect to take-off power (be it a STOL take-off or VTOL take-off).
- The landing and take-off phases have identical power requirements: with the high climb and descent angles, the power required for flight is dominated with the power for sustaining the vehicle in the air, and not that of moving it up or downwards.
- The power required for each of these phases is assumed constant. The total energy required for the mission can be calculated by multiplying the duration by the power of each phase and then adding all three.

Sizing iteration (specified cruise speed)

The sizing of the aircraft is achieved when

$$m_{tot} = m_{bat} + m_{empty} + m_{payload} = m_{bat} + k_{empty}m_{tot} + m_{payload} \quad (9)$$

Which can be rewritten as

$$0 = m_{bat} + m_{pay} + (k_{empty} - 1)m_{tot} \quad (10)$$

The battery equation gives us:

$$m_{bat} = \frac{E_{tot}}{\rho_{bat}} \quad (11)$$

With in turn E_{tot} being

$$E_{tot} = \frac{1}{\eta_p} (2E_{climb} + E_{cruise}) \quad (12)$$

$$E_{climb} = t_{climb}P_{climb} + m_{tot}gh_v = \frac{h_{climb}}{v_{climb}} \frac{(m_{tot}g)^{3/2}}{\sqrt{2\rho S_d FOM}} + m_{tot}gh_v \quad (13)$$

$$\begin{aligned} E_{cruise} &= \frac{dS_{ref}q}{\eta_p} \left(C_{d,0} + \frac{0.074}{Re^{0.2}} \right) + \\ &\quad \frac{d}{\eta_p} \left((h_c - h_v)m_{tot}g + \frac{m_{tot}^2 g^2}{\pi e b^2 q} \right) \end{aligned} \quad (14)$$

Substituting eqs. 11, 12, 13 into eq. 10, we have

$$\begin{aligned} 0 &= \frac{(m_{tot}g)^2 d}{\rho_{bat} \eta_p \eta_e \pi e b^2 q} + \\ &\quad \frac{(m_{tot}g)^{3/2}}{\rho_{bat} \eta_e} \left(\frac{2h_c}{v_c \sqrt{2\rho S_d FOM}} \right) + \\ &\quad \frac{(m_{tot}g)}{\rho_{bat} \eta_e} \left(2h_v + \frac{(h_c - h_v)}{\eta_p} \right) + \\ &\quad (k_{empty} - 1)m_{tot} + \\ &\quad m_{pay} + \frac{dS_{ref}q}{\eta_p \eta_e} \left(C_{d,0} + \frac{0.074}{Re^{0.2}} \right) \end{aligned} \quad (15)$$

Setting $x = m_{tot}^{1/2}$, eq. 15 can be rewritten as

$$0 = a_0x^4 + a_1x^3 + a_2x^2 + a_3x + a_4 \quad (16)$$

With

$$a_0 = \frac{dg^2}{\eta_p \eta_e \pi e b^2 q \rho_{bat}} \quad (17)$$

$$a_1 = \frac{1}{\rho_{bat} \eta_e} \left(\frac{2h_c g^{3/2}}{v_c \sqrt{2\rho S_d FOM}} \right) \quad (18)$$

$$a_2 = \frac{g}{\rho_{bat} \eta_e} \left(2h_v + \frac{(h_c - h_v)}{\eta_p} \right) + (k_{empty} - 1) \quad (19)$$

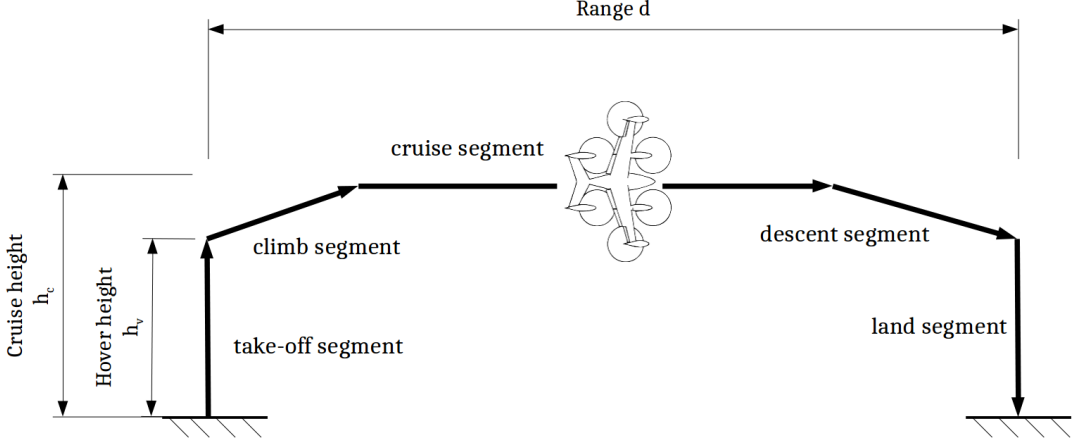


Fig. 2: Schematic of a typical eVTOL mission, showing the vertical take-off and landing segments as well as the cruise portion of the flight.

$$a_3 = 0 \quad (20)$$

$$a_4 = m_{pay} + \frac{dS_{ref}q}{\eta_p \eta_e \rho_{bat}} \left(C_{d,0} + \frac{0.074}{Re^{0.2}} \right) \quad (21)$$

The roots of eq.16 represent converged vehicles for a given mission. If the polynomial has no solution, then a vehicle for the given mission and parameters does not close. Amongst all the possible solutions to equation 16, the smallest real root is selected, in order to pick the lightest vehicle that closes for the mission in question.

Noise prediction

This part of the model is the most challenging and contains the most constraining assumptions concerning vehicle design. Nevertheless, these appear in most practical eVTOL designs:

- The propulsion system for both vertical flight and forward flight is propeller based: Two or three bladed propellers are common in the current designs, such as the volocopter Figure 3 and the Cora vehicle Figure 13 or the three bladed rotors of the airbus Vahana 4 and the V-22 Osprey 11.
- The vehicles will need to be quiet in order to be accepted by the public. Given the sound power generated by such vehicles, the metric chosen here is the peak sound power emitted. In order to correct for the human audition, the effective metric is peak dB(A) value of the vehicle. There exist many different sound metrics, but the dB(A) scale has the significant advantage that it is compatible with conceptual-level noise prediction methods such as the Gutin method, and that it is widely used, allowing for numerous comparisons, see Figure 15b



Fig. 3: Top view of the volocopter showing the 2 bladed rotor design, (Ref. 10)



Fig. 4: Picture of the Airbus Vahana flight test article, showing the 3 bladed rotors, (Ref. 11)

- Past experience (Ref. 1) has shown that a major if not the major barrier to air-taxi service deployment is community acceptance. Thus this study is focused on the outside noise of the vehicle, i.e. the noise perceived by bystanders. Noise inside the vehicle is beyond the scope of this paper. Given the focus on the noise perceived by the surrounding community and given the required cruise power, distance between noise source and by-standers, it is take-off and landing that is the most critical phase from noise perspective.

Low blade count rotor noise prediction method For this low-speed application and given the low number of blades,

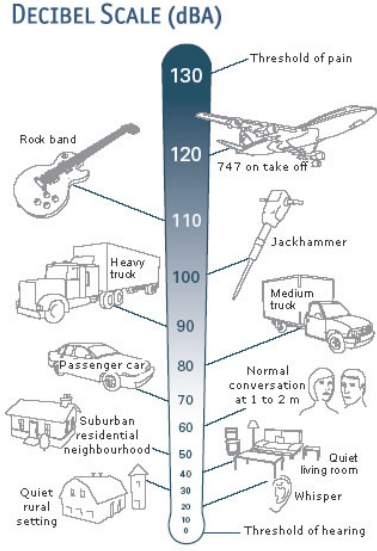


Fig. 5: Scale showing typical noise levels of everyday events (Ref. 12)

the Gutin noise model is applied to calculate the noise intensity. The Gutin method has been shown to be a good first approximation (Ref. 13) of noise for slow advancing propulsive propellers, which are defined here as being of modest diameter (flow uniform across the entire disc) and with a low blade count (not a low speed fan). The noise is calculated in two steps: the first is the computation of the root mean squared sound pressure of the first 10 harmonics (10 harmonics captures this type of noise to a large extent. Using more harmonics will show an imperceptible dB(A) increase, but not change the observations and conclusions) Using the relation of (Ref. 14) to calculate the pressure levels of each harmonic i :

$$p_{m,i} = \frac{169.3m_i BRM_i}{rS_d} \left(\frac{0.76P_h}{M_t^2} - T \cos \theta \right) J_{m_i B}(x) \quad (22)$$

The dB(A) value is calculated by adding up the pressure levels $p_{m,i}$ with the A-weighting and a normalizing pressure $P_{ref} = 20 \times 10^{-6} Pa$:

$$dB(A) = 20 \log_{10} \left(n_{prop} \sum_{i=1}^{N=10} A(f_i) \frac{p_{m,i}}{P_{ref}} \right) \quad (23)$$

The metric used is the overall sound pressure level in dB(A) perceived by a bystander at 30 m from the take-off point, with an observer angle of 110 degrees Figure .9, which is the region in which the noise is worst. The worst noise angle to the observer will depend on the configuration as well as the shielding. However, since the lift-off system will have to blow the air downward in an unobstructed fashion in order to be effective, this worst-case scenario will likely occur with any configuration. Another advantage of this particular setup for noise measurements is that some helicopter noise data is available from the National Park service (Ref. 15) which give another means of comparison. The aircraft studied in National Park Service report are the MD-900 (Figure 6) and the Bell



Fig. 6: The MD-500 quiet technology helicopter (Ref. 15)



Fig. 7: The Bell 407 helicopter (Ref. 15)

407 (Figure 7). Note that these aircraft have similar sizes and missions to the prototypical eVTOL. On take-off, the maximum sound for both aircraft was measured to be 97.2dB(A) according to (Ref. 15)

Vehicle sizing routine and parameters studied

The goal of this paper is to explore high level configuration choices. The work flows in the following steps:

- list a series of sweeps on the basic parameters of the mission to be fulfilled. In this case, the mission parameters are:
 - Payload mass, ranging from 50 kg to 500 kg
 - Range, ranging from 10 km to 100 km.
 - Cruise velocity, ranging from 150 km/h to 300 km/h

The choice of these parameters is dictated by the practical use of eVTOL aircraft, which will likely be close to

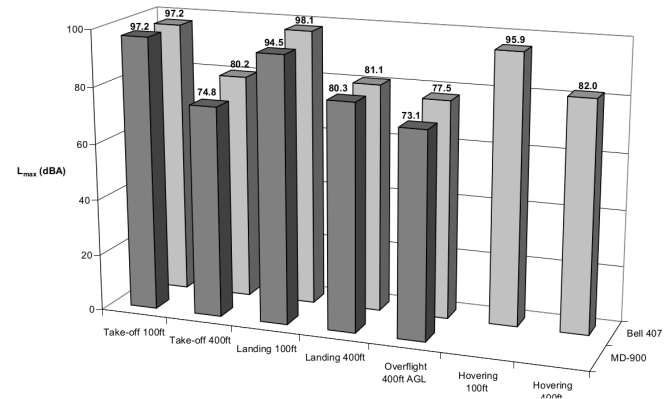


Fig. 8: The noise measurements of the Bell 407 and MD500 helicopters (Ref. 15)

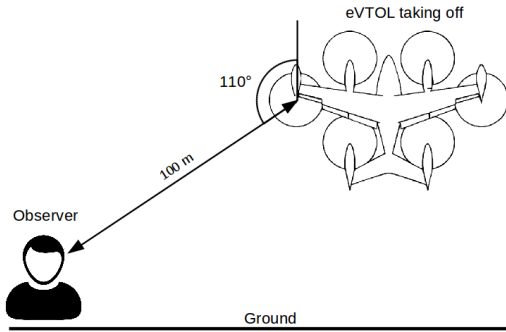


Fig. 9: Configuration in which the sound intensity is measured

the ground, removing the altitude requirement, and limited speed range since low speeds are of little practical use and higher speeds incur effects of compressibility.

In the present model, the choice of an aircraft configuration is based on two variables: the lift systems disc area S_d and the cruise lift system area (wing area) S_{ref} . In the interest of generality, these areas are normalized with respect to the footprint area. Note that in this study, both cruise lift and hover lift systems may take up the entire footprint area (like in the case of a helicopter, where the rotor accomplishes both functions). Figures 11, 14, 13 show examples of these area ratios and how the aircraft configuration may change by varying these parameters.

Aircraft	$\frac{S_{wing}}{S_{footprint}}$	$\frac{S_{disc}}{S_{footprint}}$	$\frac{S_{disc}}{S_{wing}}$
V-22 Osprey	0.053	0.404	7.622
Cora	0.11	0.14	1.27
Lilium Jet	0.12	0.05	0.41

Figures 15a, 15b show the following:

- The smaller disc areas are limited by the C-rate constraint, whereas the lower wing surfaces are limited by the lift coefficient constraint.
- For this particular mission, it seems that the Cora vehicle area ratios are most appropriate, since it is within the limit of the feasible designs, the Lilium concept requiring too much power and the scaled V-22 having a too smaller wing.
- The vehicle weight displays a sharp decrease from disc area ratios that are within the feasible C-rate area. From a practical perspective, this means that there is a disc area ratio that is not worth exceeding if practical reasons such as packaging or clearance are of interest.
- Although the decrease in MTOW is small for higher disc areas, the rate of decrease in sound intensity continues beyond the disc area fraction of 0.2. This points to the fact quiet eVTOLs have a tendency of having large lift rotor areas.

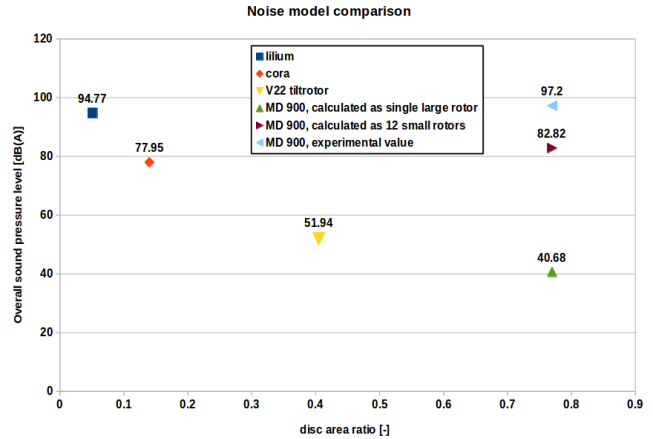


Fig. 10: Limitations of the acoustics model used: the Gutin model makes the assumption that the flow over the rotor is uniform. When the rotor size increases, the flow becomes non-uniform and higher order harmonics become a dominating contribution to overall noise, as seen in (Ref. 14). This is the reason for which the calculated V-22 osprey and MD-900 noise values are so optimistic. To afford a means of comparison, from now on all concepts will have the same number of rotors, namely 12: this number is a realistic number for eVTOL aircraft designs (as for Cora) and it slices the disc area into smaller rotors making the Gutin sound prediction more accurate. Note that despite artificially reducing the rotor size, the Gutin method still underpredicts the measured noise by 15 dBA.

- The tilt-rotor has relatively low noise: this is due to the large rotor size, which the Gutin model underestimates for the reasons cited in the paragraph concerning the noise modelling. However, the tendency to reduced noise is real: the lower disc loading of large rotors will have beneficial effects on noise. This points to the fact that quiet eVTOLs require high torque, low-speed motors. High torque propulsion systems are heavier than low torque ones, showing the importance of the trade between light and quiet propulsion systems with eVTOL configuration selection and design.
- Wing area has little effect on sound intensity. This suggests that all cruise systems may be decoupled from the rest of the aircraft design in regards to the noise signature.

As can be seen on Figures 15a, 15b, there is a region in the parameter space where the vehicle is feasible: this region is bounded by the closure of the vehicle:

- The upper limit and/or lower limit in converged MTOW, or the constraint imposed by the lift coefficient (as seen in Figure 15a: the lower space of dotted lines represents the lift coefficient limit due to the wing getting too small).
- The side limits set either

Table 1: Parameters. All elements marked by – signify the parameter is kept constant for all studies.

Value, unit	Reference	lower bound	upper bound
Vehicle parameters:			
footprint diameters, m	8	6	12
propulsive efficiency, [-]	0.7	–	–
electric drive chain efficiency, [-]	0.85	–	–
number of lift rotors, [-]	12	–	–
lift rotor figure of merit, [-]	0.7	–	–
empty weight fraction, [-]	0.65	0.55	0.75
battery energy density, [Wh/kg]	200	140	400
span efficiency, [-]	0.8	–	–
parasitic drag coefficient (w.r.t wing area)	0.03	–	–
maximum lift coefficient	1.0	–	–
maximum C-rate	10	–	–
Mission parameters:			
Range, km	75	50	150
Payload, kg	200	100	400
Cruise alt, m AGL	500	–	–
Cruise speed, km/h	250	200	320
hover height, m AGL	100	–	–
air density, [kg/m³]	1.225	–	–
dynamic viscosity, [kg/m/s]	1.78E-5	–	–
vertical climb speed, [m/s]	3	–	–

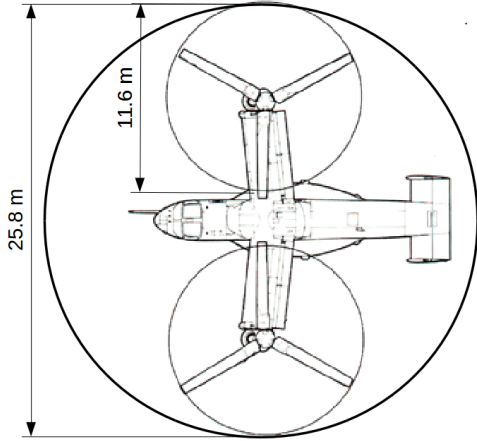


Fig. 11: Top view of the Boeing V-22 Osprey. It has a disc area of $S_d = 2\pi \left(\frac{11.6}{2}\right)^2 = 211.4\text{m}^2$. Wing area is $S_{ref} = 28\text{m}^2$

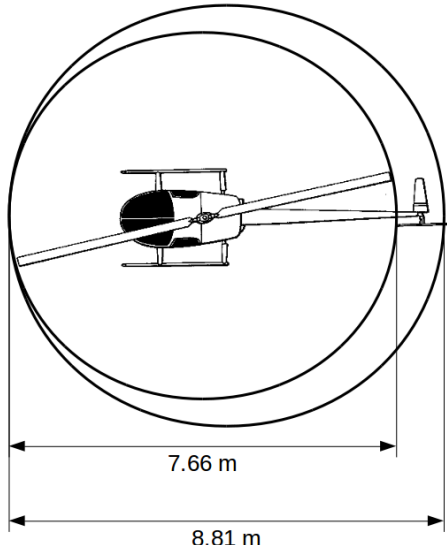


Fig. 12: Top view of the Robinson R-22. It has a disc area of $S_d = \pi \left(\frac{7.66}{2}\right)^2 = 46.1\text{m}^2$. Equivalent wing area is $S_{ref} = 46.1\text{m}^2$

- By the C-rate requirement (as seen in Figure 15a: the left-side space of dotted lines represent the region where the vehicle closes, but whose C-rate exceeds the capacity of the battery)
- Or by the rotor packing constraints themselves, since even a helicopter can not cover the entire footprint area with its rotor, as seen in Figure 12. Typical values for disc area ratios for helicopters are around 0.75.

This region of feasibility is of fundamental importance: by showing limits on disc and wing area ratios, it sets limits to which class of concept can close for a given mission. For ex-

ample, it shows that a "Lilium jet" type concept can not work for the specified mission due to the high C-rate required to take off with its small disc area ratio. The "Cora" type concept is on the limit of feasibility (if the maximum C-rate is 10), and the tiltrotor concept would be infeasible due to the excessive lift coefficient. Note however the tiltrotor case has the V-22 area ratios, and that the V-22 mission is very different from the urban air mobility mission, in particular the V-22 flies much faster, thus dropping the required lift coefficient

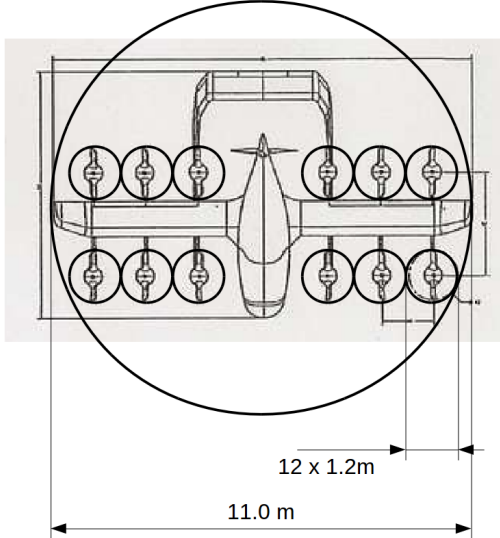


Fig. 13: Top view of the Cora air vehicle. It has a disc area of $S_d = 12\pi \left(\frac{1.2}{2}\right)^2 = 13.57m^2$. Wing area is $S_{ref} = 10.6m^2$

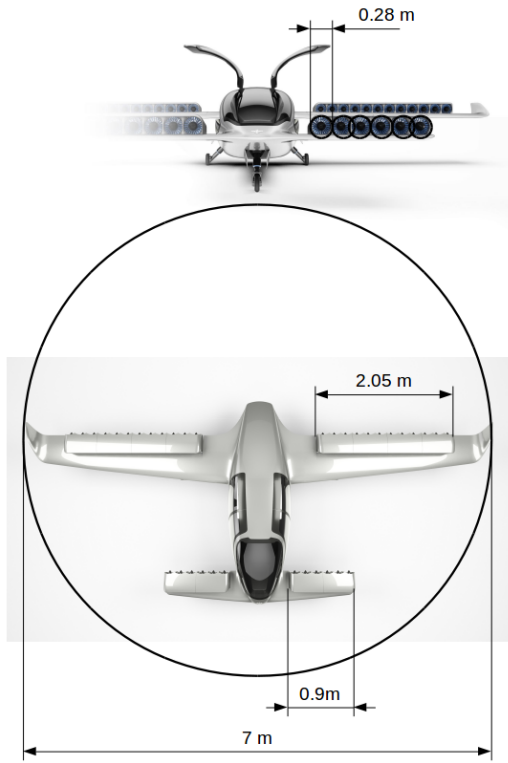


Fig. 14: Top view of the Cora air vehicle. It has a disc area of $S_d = 36\pi \left(\frac{0.28}{2}\right)^2 = 2.21m^2$. Wing area is $S_{ref} = 4.61m^2$. Full scale wing span is said to be 7 m ([...] the first 1:2 scale prototype in the final design was completed. It is the precursor to the original, and has a wingspan of 3.5m. <https://arts.eu/blog/blog-3/post/lilium-jet-electric-plane-of-the-future-the-lilium-jet-an-innovation-in-aviation-43>. Figures from lilium.com, visited on 12.10.2018

and redering the concept feasible.

The rest of this work will focus on the feasibility regions alone, in order to not overload the graphs while still capturing the insights concerning feasibility and sensitivity to different designs. Figures 16a, 16b show the feasibility regions of the cases seen in Figures 15a, 15b.

Model verification

The present model contains a few assumptions that have to be verified:

- *The hover height has little overall effect on the feasibility of an urban eVTOL aircraft:* This is shown in Figure 17: This shows that higher hover heights allow for smaller disc area ratios, which seems counter-intuitive. However, because of the greater energy requirement to lift the vehicle higher, the battery grows (as does MTOW) and thus the C-rate is reduced. Although there is a difference between which types of vehicles are feasible depending on hover height, the changes are relatively small (i.e., the class of feasible vehicles remain the same) in comparison to the parameter changes that will be discussed in the results section.
- *The parasitic drag has little effect on the feasibility of an urban eVTOL aircraft:* like the previous case, the sensitivity of feasibility to parasitic drag makes a quantitative difference, but not a qualitative one: a badly designed aircraft with 0.02 drag coefficient may weigh as much as a properly designed aircraft with as 0.04 drag coefficient.

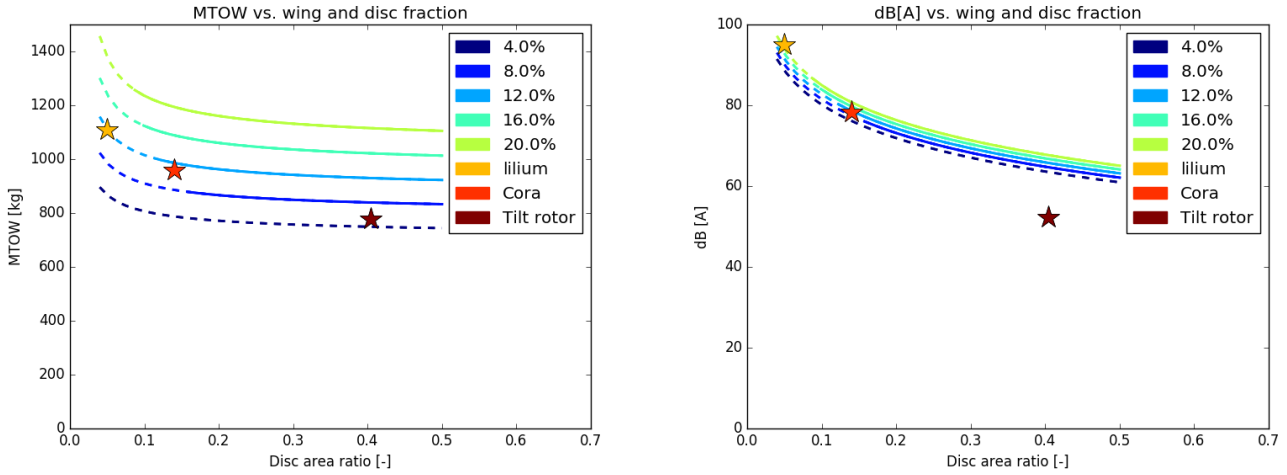
RESULTS

This section extends the observations made in Figure .15a,15b by observing:

The effect of increased payload Increased payload signifies that the design is more constrained, and the design space shrinks. This shows what kind of eVTOL aircraft are more robust to changes in mass for the urban taxi mission of interest.

The effect of decreased footprint Decreased available footprint is always a disadvantage, but it is particularly sensitive with eVTOLs, who rely on disc area to lower power consumption for lift-off.

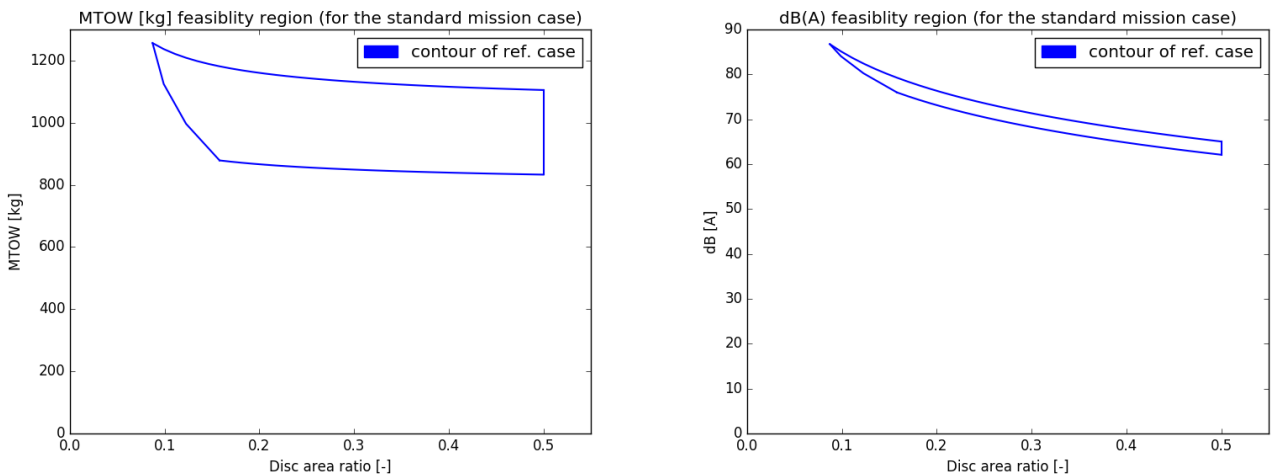
The effect of vehicle mass fraction Comments about how technological change changes the fraction of all that in non-payload or battery related. The effect of changing the empty mass fraction is qualitatively similar to that of increasing or reducing payload (see Figures 19a,19b). The insight from a concept selection perspective is that with higher empty weight fractions, larger disc areas are required, forcing the design to aircraft simialr to the helicopter or tiltrotor. One might argue that helicopters and tilt-rotors are not required anymore, since relatively recent technologies such as composite airframes improve



(a) Maximum take-off weight of an eVTOL with the reference mission depending on the wing area ratio and the disc area ratio. On the x-axis the disc area ratio is displayed, the different lines represent different wing area ratios. All solid lines are solutions that both have a C-rate in hover of less than 10 C, and a lift coefficient in cruise of less than 1.0. The dashed lines are solutions regardless of the limits on lift coefficient and C-rate. Note that both C-rate and lift coefficient are arbitrary limits. The coloring of the lines corresponds to the different wing area ratios.

(b) A-weighted sound intensity of an eVTOL with the reference mission depending on the wing area ratio and the disc area ratio. On the x-axis the disc area ratio is displayed, the different lines represent different wing area ratios. The number of blades is 2, the tip Mach is $M=0.6$. All the lines are assumed to have 12 lift rotors. All solid lines are solutions that both have a C-rate in hover of less than 10 C, and a lift coefficient in cruise of less than 1.0. The dashed lines are solutions regardless of the limits on lift coefficient and C-rate. Note that both C-rate and lift coefficient are arbitrary limits.

Fig. 15



(a) Feasibility region for the baseline vehicle and mission parameters. The area shown encloses the solid lines shown in Figure 15a.

(b) Feasibility region for the baseline vehicle and mission parameters. The area shown encloses the solid lines shown in Figure 15b.

Fig. 16

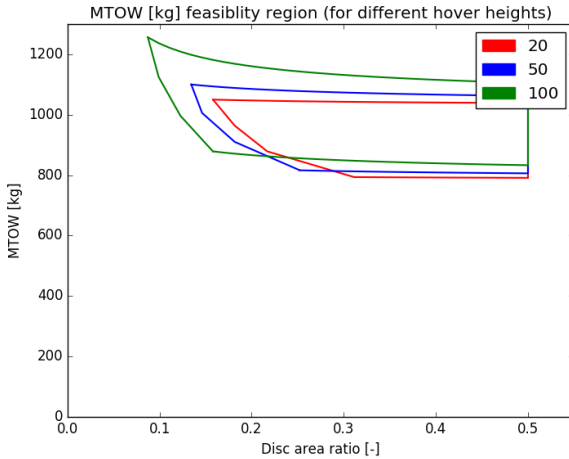


Fig. 17: Effect of the hover height (20 m, 50 m, 100m) segment on overall feasibility.

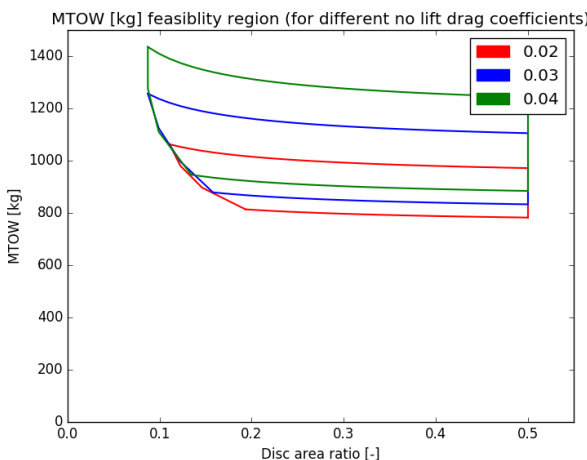


Fig. 18: Effect of the parasitic drag coefficient ($C_{d0} = 0.02, 0.03, 0.04$) on overall feasibility

mass fraction, making the multi-rotor or fan powered concepts feasible. However, distributed propulsion leads to larger airframe since the carrying structure must be spread out, such as on the Volocopter, see Figure 3. The question is whether the performance hit of a large distributed airframe is still sufficient for economic operation.

The effect of battery energy density It is often advertised that improvements in battery technology will make eVTOLs better in every way. However, as can be seen in Figures 22a, 22a increased battery energy density has diminishing returns: low energy densities produce aircraft that are too heavy to be practical, but high energy densities do not have the same amplitude in the opposite direction. It does increase the possible aircraft concept range by making smaller disc-area ratios feasible. Another approach to gain the same effect would be to increase the allowable C-rate while maintaining battery energy density constant. One of the interesting aspects of

using electric propulsion is the high power to weight ratio it is capable of delivering. Thus a high-C-rate battery combined with wet fuel cruise propulsion system might produce the best of both worlds.

Note that the effect of higher battery energy densities on noise is small. One could argue that through high battery energy densities the vehicle can be sized smaller and the vehicle may in turn be quieter, but this effect is small in comparison to the others discussed here to reduce noise.

These results show that new technologies such as distributed propulsion, composite airframes and autonomous flying enable many new possibilities for urban air transportation, physical limits remain. Also, improvements in technologies such as batteries do help, but not for all problems needed to be addressed (noise in particular) and not to the extent that papers such as (Ref. 2) may lead to believe.

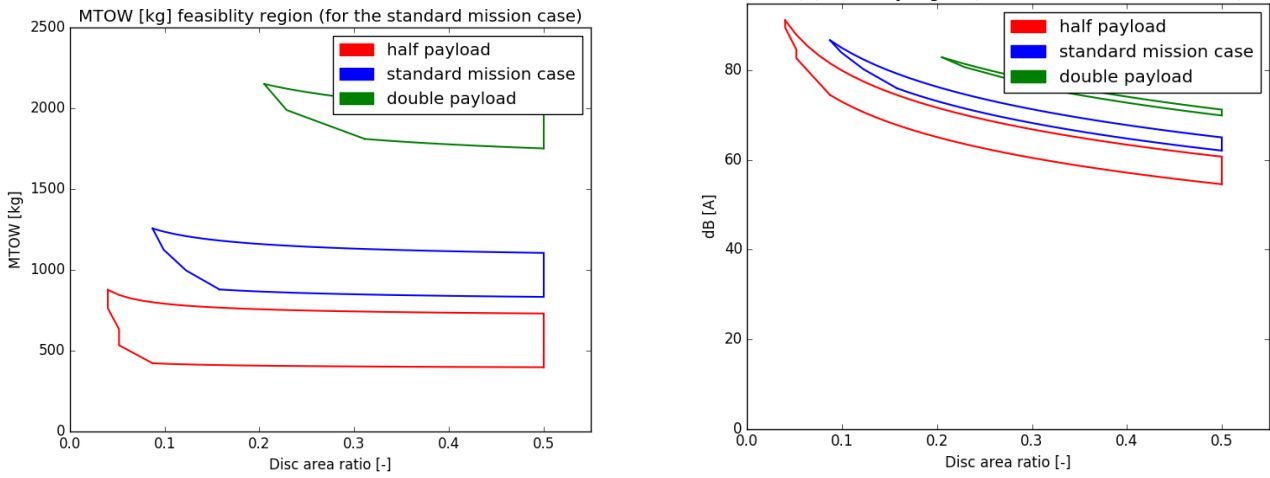
Overall, it is clear that for the ranges considered the highest performing aircraft are ones with large disc-area ratios. For the urban air-mission, disc-area ratios beyond 0.2 have diminishing returns, but below this number the performance and noise are significantly worsened. This has a direct impact on the economic viability of an eVTOL aircraft, since high performance aircraft can carry more paying customers than low performance aircraft. High disc-area ratio aircraft such as compound helicopters, gyrocopters and tilt-rotors are often not associated with eVTOL because of the good argument that many rotors are needed to provide redundancy. However the drop in performance and possible noise nuisance might render these classical concepts more attractive. To the best of the authors knowledge, few concepts have been proposed which apply technologies such as autonomy and electric propulsion tilt-rotor and helicopter like aircraft. This could prove to be a highly fruitful research direction.

CONCLUSION

-Improvement in battery technology has diminishing returns in terms of energy density. -Increasing the C-rate at equal energy density opens the possibility of closing concepts with less disc area.

-In terms of noise and performance for the UAM mission class discussed, the concept class with the greatest potential are single rotor or stacked rotor concepts, such as winged gyrocopters, compound helicopters and derivatives thereof.

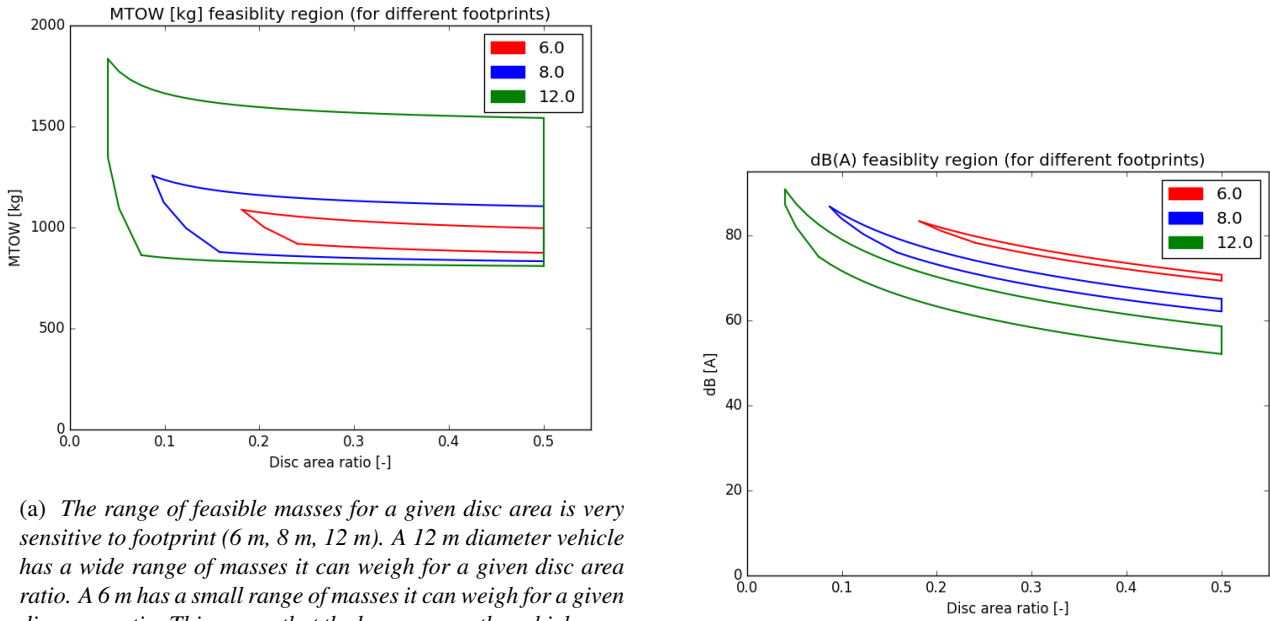
This goal of this work was to gain insight in what key parameters drive eVTOL design. The emphasis was set on removing concept-specific characteristics and thus the classification was based on a momentum theory approach, where VTOL aircraft are described by a disc-area ratio for hovering flight and a wing-area ratio for cruising flight. Using these two parameters, a sizing method was derived using basic assumptions and parameters of the vehicle. With this model, the sizing loop reduces to solving a 4th order polynomial, which allowed for sweeping of the design space defined by disc- and wing-area ratios. This allowed the mapping of feasibility regions,



(a) *Effect of varying payload (100kg, 200 kg, 400 kg) on MTOW: the payload mass has a major effect on vehicle sizing and design, which is expected. Note how higher payloads require a larger minimum disc area to be feasible, forcing the conceptual design toward concepts similar to tilt-rotors and beyond. The kinks seen in the half payload case (red) are due to the discretization of wing area ratios the sweeps were conducted with.*

(b) *Effect of varying payload (100kg, 200 kg, 400 kg) on take-off noise: The results reflect the tendencies of Figure 19a. Note however that the noise generated by the large payload aircraft collapses into a narrow noise band. This behaviour is seen when the disc-loading increases (as with Figure 20b), suggesting there is little design flexibility to reduce take-off noise with vehicles with high-disc loadings.*

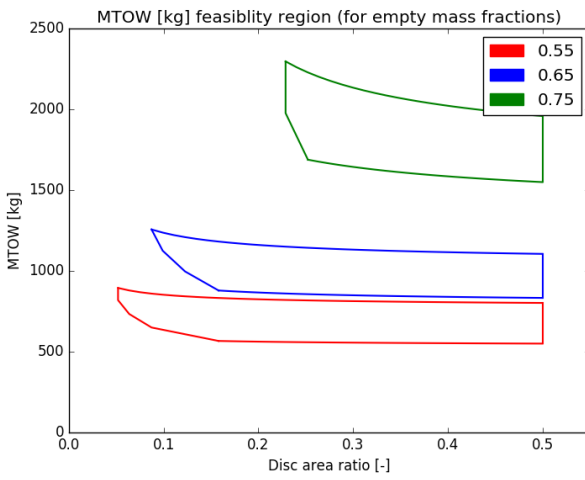
Fig. 19



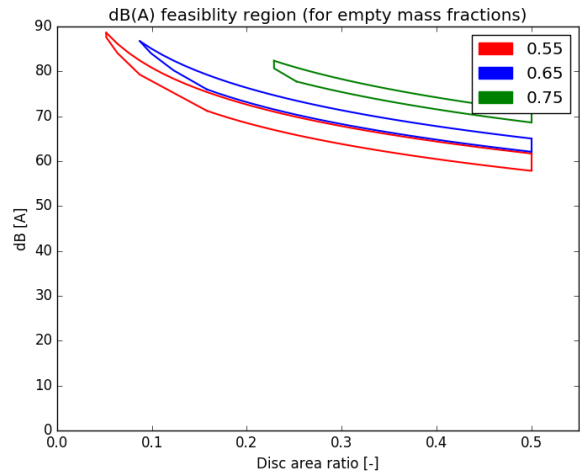
(a) *The range of feasible masses for a given disc area is very sensitive to footprint (6 m, 8 m, 12 m). A 12 m diameter vehicle has a wide range of masses it can weigh for a given disc area ratio. A 6 m has a small range of masses it can weigh for a given disc area ratio. This means that the larger space the vehicle may occupy, the less sensitive it is to weight creep. A small footprint vehicle is thus riskier to develop, since a little weight creep will make it impossible to close. The range of feasible disc area ratio is very sensitive to footprint: Because of the power limit on the battery, there is an inferior limit on the disc area. Thus the smaller footprint vehicle needs a relatively high disc area ratio to be feasible, favoring concepts with good rotor area ratios such as helicopter like vehicles.*

(b) *The footprint has one of the largest effects on overall sound pressure of the parameters explored in this paper. Note that the sound model used favors large rotors over small ones, so the effect of increased footprint will be mitigated once the rotors become large enough to behave less like a vertical propeller and more like helicopter rotor. Despite this effect, this result suggests that increased footprint has a large beneficial effect on sound and should not be neglected during concept selection.*

Fig. 20

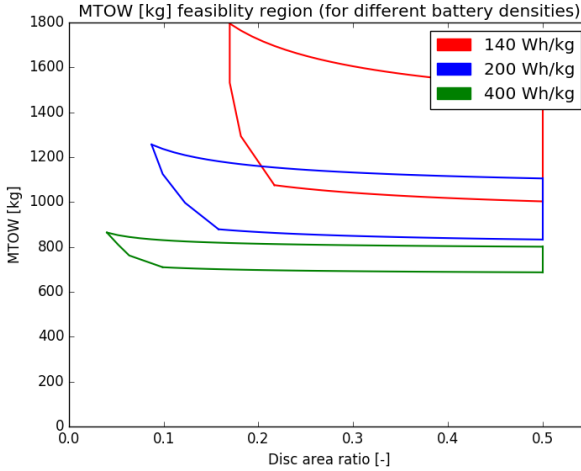


(a) The mass fraction range used here is $k_{empty} = 0.55, 0.65, 0.75$. The effects of mass fraction are qualitatively similar to those of payload: as expected, they have a major impact on vehicle feasibility and mass for a given mission. As a insight for concept selection, this shows that higher airframe mass fractions force concepts to use larger disc-area ratio concepts, such as those seen in helicopters and tilt-rotors.

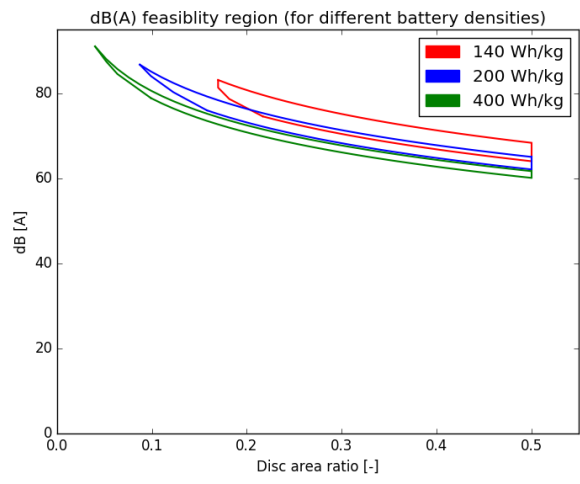


(b) The mass fraction range used here is $k_{empty} = 0.55, 0.65, 0.75$. The effect of changing the mass fraction does not have unexpected results on sound, it is qualitatively similar to changing payload, see Figure ??, except that the sound range for a given mass fraction are similar. The higher empty mass fraction band has similar width that that of the lower mass fractions, suggesting that there is the same design flexibility to improve noise for higher empty mass fraction than there is for lower empty mass fractions.

Fig. 21



(a) When battery energy density is improved, smaller disc area ratios become possible because the available power goes up due to improved capacity of the battery, making concepts possible that have little disc-area available. Conversely, this shows that a reduced battery energy density or C-rate will make small disc-area concepts unfeasible. Another interesting aspect is the diminishing returns of increased energy-density on overall vehicle mass: small energy densities have a large range of feasible MTOWs because the increased energy available by adding a given amount of battery serves only to carry that added amount itself. If energy density is increased, the dominant mass becomes the aircraft empty weight, and increased battery energy density is of diminishing use.



(b) Although it might be argued that increased battery energy density will allow lower noise aircraft through more efficient design, this result shows that **improved battery energy density has little effect on noise**. For radically different battery technologies, the areas showing the results overlap. This result shows again that improved noise comes from lowering disc loading, and the MTOW. However, as seen in Figure .22a

Fig. 22

which were used to illustrate what concept classes were feasible given a particular mission, in this case the 2 passenger urban air taxi type.

The results show that in this case:

- The height of hover out phase of the mission and the parasitic drag coefficient have an effect on feasibility, but that it is not as pronounced as other parameters such as footprint size. Note that the reference value chosen for parasitic drag is that of a general aviation airplane (Cessna 172)
- Disc-area ratio plays a large role in aircraft performance, especially in the region below 0.2. Beyond 0.2, the disc-area ratio has diminishing returns.
- Compact and quiet vehicles require large disc-area ratios in order to be feasible.
- The increase in battery energy density has diminishing returns, and does not improve overall aircraft performance to show any significant gain in noise.
- Increase in battery energy density allows smaller disc-area ratio airplanes to be feasible. Increasing the C-rate of the batteries has the same effect.
- In terms of noise and performance for the urban air mobility mission class discussed, the concept class with the greatest potential are large rotor area concepts, such as helicopters, winged gyrocopters, compound helicopters and derivatives thereof.

Author contact: Olivier Cornes, cornes.olivier@aurora.aero

APPENDIX

Appendix A: Empty mass fractions, see Table 2

EMPTY WEIGHT FRACTIONS

ACKNOWLEDGMENTS

The author would like to thank Robert Parks and Francesco Giannini for their helpful advice as well as Aurora Swiss Aerospace.

REFERENCES

¹Parker Vascik. *Master Thesis Systems-Level Analysis of On-Demand Mobility for Aviation*. PhD thesis, MIT, 2017.

²Nikhil Goel Jeff Holden. Fast-Forwarding to a Future of On-Demand Urban Air Transportation, 2016.

³Joby aviation main website. <http://www.jobyaviation.com/>. Accessed: 2019-01-16.

⁴Vahana webiste. <https://www.airbus.com/newsroom/press-releases/en/2018/02/vahana--the-self-piloted--e-vtol-aircraft-from-a--by-airbus--succ.html>. Accessed: 2019-01-16.

⁵Robert Moorman. Helicopter noise: The peoples perspective long island and chicago. *Vertiflite*, 1(2):28–30, 2 2015.

⁶Aston martin volante vision. <http://evtol.news/aircraft/aston-martin-volante/>. Accessed: 2019-01-16.

⁷Cessna performance measurements. <http://temporal.com.au/c172.pdf>. Accessed: 2019-03-26.

⁸Wayne Johnson. *Helicopter Theory*. Princeton University Press, Princeton, NJ, 1980.

⁹Cora main website. <https://cora.aero/>. Accessed: 2019-01-16.

¹⁰Volocopter top view (smithsonian magazine). <https://www.smithsonianmag.com/innovation/photos-rise-volocopter-180949828/>. Accessed: 2019-03-26.

¹¹Flight test article of airbus' vahana (vertical). <https://www.verticalmag.com/news/vahana-project-ramping-flight-tests/>. Accessed: 2019-03-26.

¹²db(a) scale example from the cafe foundation. cafe.foundation/blog/wp-content/uploads/2014/06/ahuja-decibel-scale.jpg. Accessed: 2019-03-26.

¹³M. Kotwicz Herniczek D. Feszty S. Meslioui J. Park. Applicability of early acoustic theory for modern propeller design. *AIAA aviation forum*, (23), 2017.

¹⁴Donald W.Kurtz Jack E. Marte. A Review of Aerodynamic Noise From Propellers, Rotors, and Lift Fans, 1970.

¹⁵Laura Levy Sarah Falzarano. Sound levels of helicopters used for administrative purposes at Grand Canyon National Park, 2007.

Table 2: Empty weight fractions from Figure 1

	empty weight [kg]	MTOW [kg]	empty mass fraction
UAVs			
Scan eagle	14.05	22.05	0.64
Arcturus T20	50.00	84.09	0.59
Arcturus T16	25.00	38.64	0.65
Bell eagleeye tiltrotor	590.91	1022.73	0.58
AAI shadow 200	84.55	170.45	0.50
GNAT 750	254.55	518.18	0.49
I-GNAT	386.36	704.55	0.55
MQ-1B predator	513.64	1022.73	0.50
Reaper	2227.73	4770.00	0.47
global hawk	6795.45	14659.09	0.46
Blackjack	36.82	61.36	0.60
Orion	2350.00	5090.91	0.46
Hunter	659.09	886.36	0.74
Krossblade	1.61	2.00	0.80
VXP	4575.00	5529.55	0.83
Flexrotor	12.82	21.82	0.59
AAI shadow 600	159.09	265.91	0.60
AAI shadow 400	115.45	211.36	0.55
GA aircraft			
Cirrus SR22	1011.36	1636.36	0.62
Cessna 400 (Columbia)	1136.36	1636.36	0.69
Pipistrel Panthera	816.82	1317.73	0.62
Lancair IV	1000.00	1613.64	0.62
Diamond DA42	1253.64	1703.64	0.74
Diamond DA40	797.73	1202.27	0.66
Liberty XL2	527.27	795.45	0.66
Cirrus SR20	966.36	1386.36	0.70
Cessna 350 Corvalis	1045.45	1545.45	0.68
Cessna Citation Latitude	8480.00	14454.55	0.59
Gulfstream G-100	6227.27	11204.55	0.56
Hondajet	3274.09	4818.18	0.68
Pilatus PC 24	4975.45	8021.82	0.62
CubCrafters Xcub	552.73	1045.45	0.53
Vans RV10	754.55	1227.27	0.61
Vans RV14	563.64	931.82	0.60
Vans RV9	467.27	795.45	0.59
Flight Design CT	318.64	473.64	0.67
Tecnam P2008	354.55	601.36	0.59
Pipestrel Sinus 912	284.55	545.45	0.52
pipestrel Virus SW100	289.55	600.91	0.48
Remos GX	320.45	600.00	0.53
cessna 172R	768.64	1113.64	0.69
Piper cherokee	545.91	977.27	0.56
snowgoose	272.73	636.36	0.43
MQ8B firescout	942.27	1431.82	0.66
VTOL			
Bell eagleeye tiltrotor	590.91	1022.73	0.58
Krossblade	1.61	2.00	0.83
Flexrotor	12.82	21.82	0.59
MD900	1531	3129.00	0.49
V22	15032	23859.00	0.63
Hawker siddely harrier	6140	11430.00	0.54
Robinson R22	399	622.00	0.64
Bell 280 Valor	15000	26000.00	0.58
XV15	4574 15	6000.00	0.76
AW609	4765	7620.00	0.63
XV3	1907	2218.00	0.86